

## An open-loop control algorithm of the active reflector system of FAST

Hui Li (李辉) and Peng Jiang (姜鹏)

National Astronomical Observatories, Chinese Academy of Sciences, Beijing 100101, China; [lihui@nao.cas.cn](mailto:lihui@nao.cas.cn),  
[pjiang@nao.cas.cn](mailto:pjiang@nao.cas.cn)

CAS Key Laboratory of FAST, National Astronomical Observatories, Chinese Academy of Sciences, Beijing 100101, China

Received 2019 April 1; accepted 2019 June 3

**Abstract** An open-loop control algorithm is put forward for continuous paraboloid deformation of the active reflector system of the Five-hundred-meter Aperture Spherical radio Telescope (FAST). The method is based on a calibration database and interpolation in 2D spatial domain and temperature domain, respectively. It is completely independent of real-time measurement of cable nodes so that it has advantage of working all-weather and no additional electro-magnetic interference (EMI). Furthermore, its control accuracy can be effectively improved via reasonable layout of the calibrated paraboloids and increasing calibration accuracy. Meanwhile deformation safety is considered via calibration as well. Finally its control accuracy is also confirmed via site measurements of paraboloid deformations.

**Key words:** Astronomical instrumentation: methods and techniques — methods: data analysis — methods: numerical

### 1 INTRODUCTION

The Five-hundred-meter Aperture Spherical radio Telescope (FAST), nicknamed “Sky Eye of China,” has attracted considerable attention thanks to its capability to search the depths of the cosmos. FAST is the largest single dish and the most sensitive radio telescope with Chinese own intellectual property. Its main construction and the installment of instruments were completed in September, 2016, it has since been in the commissioning phase, as shown in Figure 1.

As a large and complicate telescope, FAST consists of four main systems, including the active reflector, the feed support, the measurement and control, and the feed receivers. The active reflector system is used to form 300 m aperture paraboloid and collect in such huge area very faint radiation from the sky, which generally determines very high sensitivity of FAST (Nan 2006; Qiu 1998). It can be further decomposed as steel structures (the 500 m ring girder and 50 pillars), a flexible cable-net structure, 4450 reflector elements and 2225 actuators. The flexible cable-net and actuators are the key units to complete paraboloid and spherical deformations.

As FAST is observing and pointing to a star, its trajectory needs to be tracked due to self-rotation of the Earth.

Consequently, deformation of the cable-net is a continuous process of switching among a set of paraboloids. During this process, 2225 actuators have to drive their corresponding cable nodes in coordination so that a movable paraboloid tracking star can be formed at the right positions and the right time. The shape accuracy of paraboloid (here a statistical value based on position errors of  $\sim 700$  cable nodes) is required better than 5 mm in root mean square (RMS). Deformation control is involved in a great number of nodes and transfer of mass information at a cycle every 0.5 – 1.0 s. This means the controller has to read continuously the current actuator positions, calculate the next increments and send them to the corresponding actuators at each control cycle. A close-loop control method based on laser measurement seems to be a candidate and it is tried on site because of its large measurement range ( $> 300$  m) and excellent accuracy ( $\sim 1$  mm RMS). A total of 10 Leica laser total stations are available for parallel measurement to get the coordinates of cable nodes within paraboloid as shown in Figure 2. They are sent to the controller as feedback information by which the next incremental positions are calculated (Zhu 2012). However, this method works very slowly in that it takes 30 minutes to finish a complete measurement, which is much greater than the required cycle time. This method is also greatly limited



Fig. 1 Overview of FAST.

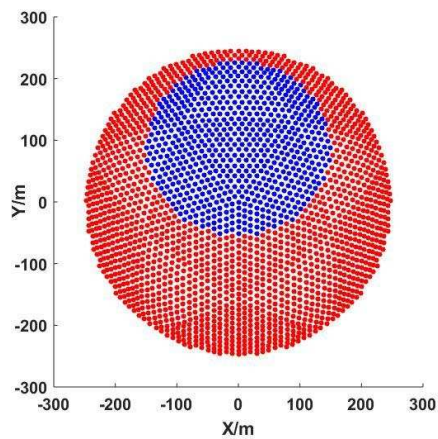


Fig. 2 2225 targets for laser measurement of the reflector system.

by weather and electro-magnetic interference (EMI), so it is not always reliable for a radio telescope.

A new open-loop method is then put forward in this paper to crack these problems. This method does not pursue real-time position measurement of cable nodes any longer, so it avoids the risks of timeout, bad weather and additional EMI. On the contrary, it builds up at first a database via recording the calibrated standard paraboloid deformations of the cable-net. The shape of each standard paraboloid is then measured and adjusted so that its shape accuracy can meet the requirement, so called de-

formation calibration. Each standard paraboloid is tied up with a group of actuator positions that are recorded in the database. For a given paraboloid, interpolation can then be applied in the database to calculate its corresponding actuator positions.

In the following sections the authors introduce first the configuration of the active reflector system and the characteristics of deformations why the open-loop control is suitable. Then, some assumptions are put forward in favor of open-loop control. The detailed algorithm is formulated with its interpolation accuracy demonstrated in a com-

putation example. Furthermore, some steps are considered on structural safety and accuracy improvement. Finally, an example on site is given.

## 2 CONFIGURATION

The flexible cable-net structure, as shown in Figure 3, can be further decomposed as a cable mesh consisting of 6670 main cables and 2225 down-tied cables most of which are along radial directions vertical to the mesh plane. Each down-tied cable is connected with a hydraulic actuator which drives to change mesh shape. It is easy for the controller to read current pressure and stroke of each actuator. The former indicates status of cable tension that is useful in monitoring structural health. The latter is closely related with the current position of cable node, hence regarded as control reference.

The cable mesh is further partitioned as about 4450 nearly orthogonal triangles with a reflector element mounting and sliding freely on the plates of cable nodes (Shen et al. 2010; Zhu et al. 2017; Jiang et al. 2017, 2013). Once the cable mesh forms a 300 m aperture paraboloid, all the reflector panels within the aperture fit a close paraboloid as well. Because the surface shape of reflector element is a sphere, fitting strategy is studied on its optimal curvature radius (Qian 2007), dimension and position of reflector element (Gan 2010), or even different surface shape (Xue et al. 2015). Offsets of real shape deviating from ideal paraboloid may exist. Here only the out-of-plane offset, also called shape error, is taken into account. It is made up of a group of factors and can be written as

$$\delta = \sqrt{\delta_1^2 + \delta_2^2 + \delta_3^2 + \delta_4^2}. \quad (1)$$

Here the symbol  $\delta_1$  represents errors of reflector panel itself, like error of designed shape, manufacturing error, thermal error, wind-induced deformation and so on. The symbol  $\delta_2$  and  $\delta_3$  represent measurement error and measurement reference error respectively. The symbol  $\delta_4$  is the error statistics of positions of  $\sim 700$  cable nodes within paraboloid aperture.  $\delta_1$ ,  $\delta_2$  and  $\delta_3$  are constants determined by panel and laser measurement, with values of 3.8 mm, 2.0 mm and 1.0 mm respectively (Jiang et al. 2019). If the required shape error  $\delta$  is set less than 6 mm,  $\delta_4$  must be less than 5 mm according to Equation (1). It is the critical requirement that deformation control of the cable mesh has to meet.

## 3 ALGORITHM OF OPEN-LOOP CONTROL

### 3.1 Assumptions on Open-loop Control

Some assumptions are given as the application base of open-loop deformation control of the cable-net. First, the

cable-net together with its supporting girder and pillars as a whole works as an ideal elastic structure. This means that special structural deformation or shape can be uniquely mapped to special load and vice versa. The same status can be repeated by the structure if the same load is imposed. That is to say the structure can remember and recall previous deformations. This assumption is also verified by long-term measurement tests of the active reflector system (Zhu & Zhang 2010). Second, the cable-net's normal transition from one shape to another is mathematically continuous. There should be no sudden jump of actuator pressure and actuator stroke on any intermediate status. The assumption puts it mathematically possible to employ interpolation method. Finally, the continuous deformation of the structure is so slow during observation that the process can be regarded as quasi-static. This assumption is reasonable in that the maximal actuator speed is less than  $0.8 \text{ mm s}^{-1}$  in the tracking mode and  $1.6 \text{ mm s}^{-1}$  in the slewing mode. Hence, the process can be divided into a group of discrete paraboloid deformations independent of dynamics.

Based on the last assumption, it is clear that the key of open-loop control algorithm is how to obtain quickly and accurately the actuator strokes corresponding to a given paraboloid deformation. The calculation results are then set as the object stroke. Their difference according to the current feedback strokes can be sent to the PLC as the next execution. The open-loop control algorithm works because the process repeats for each discrete paraboloid.

### 3.2 Standard Paraboloid and Zone Discretization

For the description convenience of a paraboloid, three variables are indispensable, including 2D position of its apex and the ambient temperature as structural deformation happens. It can be imagined that all possible positions of paraboloid apex construct a trajectory sphere. Its curvature radius is nearly equal to that of the base sphere, as shown in Figure 4. Of course they share the same spherical center. The field angle of the trajectory sphere is 80 degrees, 2 times as the maximal zenith angle designed by FAST. Hence two independent spherical coordinates, zenith and azimuth angle, are applied in denoting a paraboloid.

For the convenience of interpolation, a number of standard or calibrated paraboloids are needed. These standard paraboloids are set with special apex positions and ambient temperature. Deformation is known for each of such paraboloids. That is, the 2225 actuator strokes are calibrated regarding to the desired shape accuracy. Hence the object strokes are related with the object paraboloid deformation. All of the apexes of these standard paraboloids should be distributed as smoothly as possible for good interpola-

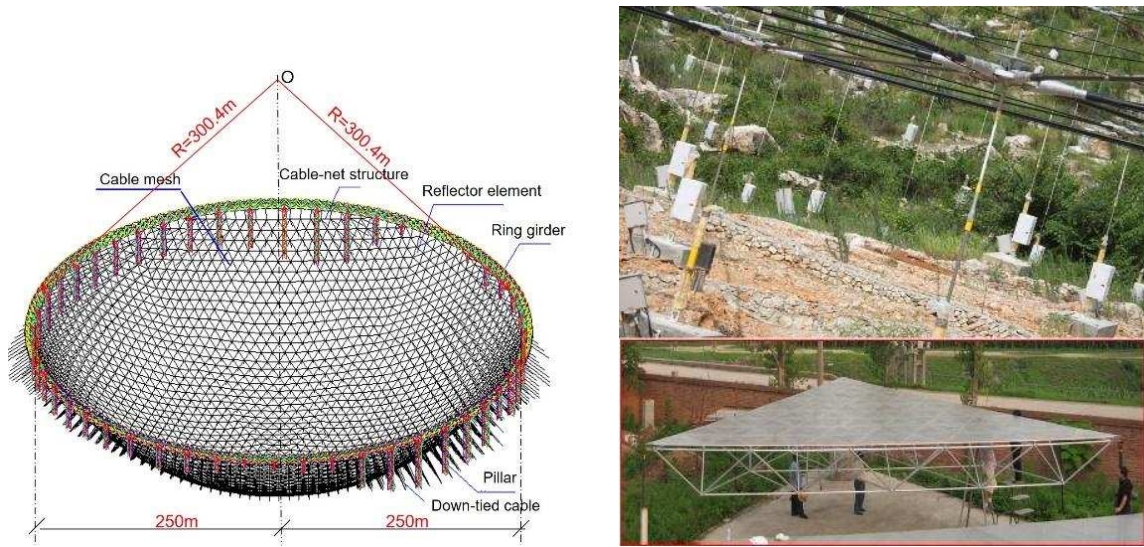


Fig. 3 The active reflector system of FAST.

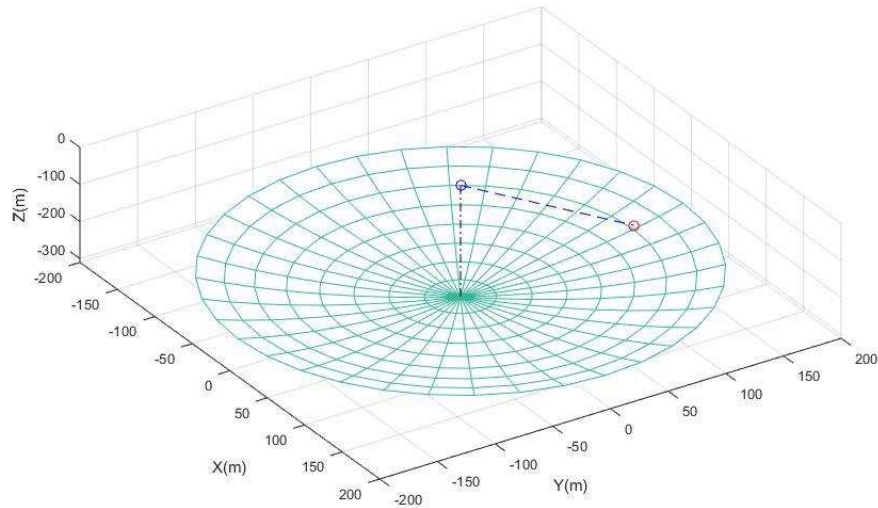


Fig. 4 Trajectory sphere of movable paraboloid.

tion accuracy everywhere. Hence the whole interpolation domain are partitioned by them as many subdomains, so called zone discretization, which happens not only in the spatial domain but in the temperature domain. Because the spatial domain is different from the temperature domain, it is advised that the zone discretization should be done separately. In the former a kind of triangular subdivision is applied according to standard paraboloids, as shown in Figure 5. The sphere is meshed by about 2000 spherical triangles with nearly the same length of 3 arc edges. Each triangle has six nodes, three of which are triangular apexes and the other are three edge midpoints. In the latter a set of discrete temperature points is given.

### 3.3 Formulation of Interpolation

Corresponding to the discretization strategy, the interpolation algorithm also consists of two steps. A first interpolation in the triangular domain is done while the ambient temperature is set constant. Then this work is repeated at each discrete temperature to get a set of intermediates as the next standard paraboloids. At last interpolation in the temperature domain is carried out to get the final interpolation results.

#### 3.3.1 Triangular domain

Figure 6 shows an arbitrary spherical triangle,  $\triangle 123$ , selected from the above subdivision with its three apexes

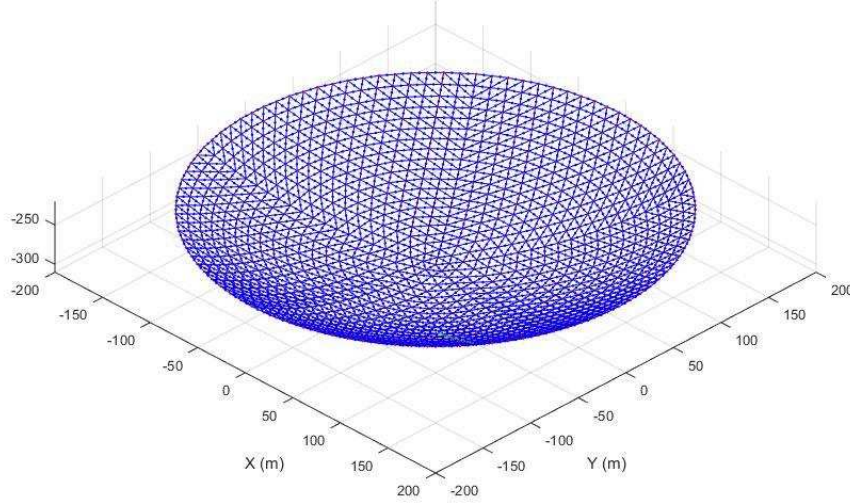


Fig. 5 Discretization mesh based on spherical triangle.

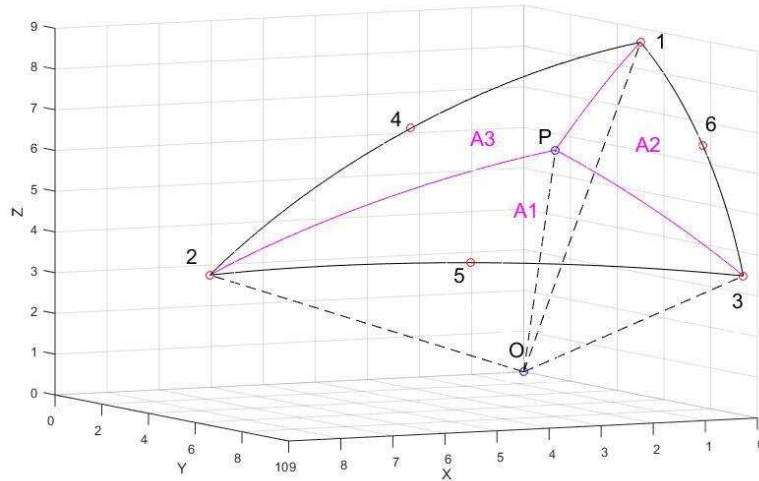


Fig. 6 Interpolation in 6-node spherical triangle.

and three edge midpoints named 1~6, respectively, each of which represents an apex of standard paraboloid. Here, a better interpolation accuracy is anticipated via 6-node triangle. Point  $P$  denotes an apex of arbitrary paraboloid within the triangular domain. For the convenience of denoting the position of  $P$ , a kind of area coordinate, namely  $L_1, L_2$  and  $L_3$ , is introduced in the following equation

$$L_i = A_i/A_0, i = 1, 2, 3. \tag{2}$$

Here the symbol  $A_0$  is area of the spherical triangle  $\triangle 123$ ; the symbols  $A_1, A_2$  and  $A_3$  are areas of the three child triangles,  $\triangle 2P3, \triangle 1P3$  and  $\triangle 1P2$ , respectively. The area of spherical triangle  $A_0$  can be calculated using the following

equation

$$A_0 = (\angle 1O2 + \angle 2O3 + \angle 3O1 - \pi) R^2. \tag{3}$$

Here  $R$  is the curvature radius of the trajectory sphere;  $O$  is the spherical center;  $\angle 1O2$  is the field angle of arc edge  $\widehat{142}$  and so on. Hence the areas  $A_1, A_2$  and  $A_3$  can also be calculated similarly. So point  $P$  can be denoted as  $P(L_1, L_2, L_3)$ . It can be proved that there is a unique mapping between the point  $P$  and the three area coordinates. Of course only two of the three area coordinates are independent. They satisfy an equation as follows

$$L_1 + L_2 + L_3 = 1. \tag{4}$$

$L_1 = 1$  means that  $P$  and Apex 1 share the same position, and so on. Based on the three area coordinates, the interpo-

lation equation on Point  $P$  in a 6-node triangular domain can be written as follows

$$\left\{ \hat{S}(P, T_j) \right\} = \sum_{i=1}^6 \Phi_i \left\{ \hat{S}(P_i, T_j) \right\}. \quad (5)$$

Here  $T_j$  is the  $j$ th discrete ambient temperature; the vector  $\left\{ \hat{S}(P, T_j) \right\}$  represents 2225 actuator strokes corresponding to the paraboloid deformation with its apex at  $P$  and under the temperature  $T_j$ ;  $\left\{ \hat{S}(P_i, T_j) \right\}$  represents 2225 calibrated actuator strokes corresponding to the  $i$ th standard paraboloid deformation;  $\Phi_i$  is the  $i$ th shape function for interpolation in 6-node triangle. This can be written as follows (Wang 2003)

$$\Phi_i(L_1, L_2, L_3) = \begin{cases} L_i(2L_i - 1), & i = 1, 2, 3 \\ 4L_{i-3}L_{i-2}, & i = 4, 5 \\ 4L_3L_1, & i = 6. \end{cases} \quad (6)$$

It is clear that the shape function is quadratic.  $\Phi_i$  is equal to 1 at the  $i$ th apex or midpoint, but 0 at other apexes or midpoints. Substituting Equation (6) into Equation (5) completes the interpolation calculation of 2225 actuator strokes for the paraboloid deformation  $P$  in triangular domain.

### 3.4 Calibration and Database

A group of cubic splines are set up as the 1D interpolation functions of the temperature domain. The equations are written as follows (Ahlberg et al. 1967)

$$\psi_j(T) = a_j + b_j(T - T_j) + c_j(T - T_j)^2 + d_j(T - T_j)^3, \quad (7) \\ j = 1 \sim N - 1.$$

Here  $a_j$ ,  $b_j$ ,  $c_j$  and  $d_j$  are the coefficients of the  $j$ th spline;  $N$  represents the number of discrete temperatures;  $T_j$  is the  $j$ th discrete temperature. The  $j$ th interpolation function  $\psi_j(T)$  is defined in the  $j$ th temperature interval ( $[T_j, T_{j+1}]$ ). It should be second-order differentiable and continuous at both ends of the interval. Assuming that the temperature difference  $h = T_{j+1} - T_j$  is a constant for any subscript  $j$ , the condition can be written mathematically as follows (Ahlberg et al. 1967)

$$\begin{cases} a_j = \psi_j(T_j) \\ a_j + hb_j + h^2c_j + h^3d_j = a_{j+1} \\ b_j + 2hc_j + 3h^2d_j - b_{j+1} = 0 \\ c_j + 3hd_j - c_{j+1} = 0 \end{cases}, j = 1 \sim N - 1. \quad (8)$$

These equations can be further simplified after elimination of redundant unknowns as follows

$$c_j + 4c_{j+1} + c_{j+2} = 3[\psi_{j+2}(T_{j+2}) + \psi_j(T_j) \\ - 2\psi_{j+1}(T_{j+1})]/h^2, \quad (9) \\ j = 1 \sim N - 2.$$

Here the only unknowns are  $c_j$ , because the value of shape function is known at the discrete temperature  $T_j$ ,  $\psi_j(T_j) = \hat{S}(P, T_j)$ . It is worth noting that the number of unknowns is  $N$ , greater than that of equations ( $N - 2$ ). Two free boundary conditions are introduced to make the equations complete. So they can be expressed as

$$c_1 = c_N = 0. \quad (10)$$

These boundary conditions are selected for the purpose of simplification if the both ends of temperature domain are far away enough from the core area. Solving Equations (9) and (10) gets the coefficients  $c_j$ . Substituting them into Equation (8) can further get  $b_j$ ,  $c_j$  and  $d_j$ . Therefore based on Equation (7) we can obtain the final interpolation of the 2225 actuator strokes as follows

$$S(P, T) = \psi_j(T), T_j \leq T \leq T_j + 1, \\ j = 1 \sim N - 1. \quad (11)$$

During the process, the program may first tell which interval the input temperature belongs to, and then apply Equation (11) to complete the interpolation.

### 3.5 Calibration and Database

There are a set of influences on interpolation accuracy. The most significant one may be the actual shape accuracy of standard paraboloid. It should be tested and confirmed via a measurement or high-decision simulation, so called calibration process. Normally calibration method via measurement on site is applied. In the process the initial actuator strokes related with a standard paraboloid are sent to the controller to get the real deformation of the cable-net structure. Then, the actual positions of all cable nodes within paraboloid aperture are obtained via laser measurement. They are compared with the ideal paraboloid. The shape error is calculated and changed into incremental strokes for the next shape adjustment. The process repeats until the shape error is less than a critical value  $\epsilon$ . The 2225 actuator strokes are then recorded in a database together with the paraboloid position and ambient temperature.

This calibration on site can give a satisfactory shape accuracy for standard paraboloids. However, it is greatly limited by weather due to laser measurement. In addition, the ambient temperature is not always able to vary as expected. Hence it may take a long time to build the database if all the standard paraboloids are calibrated via this method. A new calibration method based on finite element (FE) simulation is then developed, also called virtual calibration. In the method, a finite element model is built including all the important structural units of the reflector system. such parameters like paraboloid position and ambient temperature are input into the model and deformation of the cable-net is simulated to calculate all actuator

strokes related to the paraboloid. It is clear that relatively short time is needed disregarding measurement on site. However the simulation accuracy of the model itself needs to be tested and confirmed. On many occasions simulation results are necessary to be compared with the actual measurement so that the model can be updated.

The final calibration method may be a combination of the above two. First, a few calibrations on site are necessary. Some typical standard paraboloids should be carefully selected so that the recorded data can cover all possible deformations. Then, the data provide a base for the next updating of the simulation model. Finally, virtual calibration are applied in a full range of the interpolation zone so that a complete database can be built for the interpolation.

The database consists of three main parts. One is a vector of 2225 calibrated actuator strokes corresponding to the base sphere. It is the reference surface of zero that can only be calibrated on site. The second holds over a list of discrete temperatures and the information of spatial discretization, including a topological table and a coordinate table. The former is in memory of all 6-node spherical triangles, identifier of standard paraboloid and discrete temperatures. The latter stores the positions of all standard paraboloids. The third is the stroke table, a 3D matrix storing all calibrated actuator strokes. The first dimension represents identifier of actuator. The other two dimensions represent identifier of standard paraboloid and discrete temperature respectively.

### 3.6 Considerations on Interpolation Accuracy

It is clear that the total control errors can be decomposed into two parts, namely interpolation error and calibration error. The former is mathematically related with the number of standard points once interpolation functions are selected. The latter is determined by measurement accuracy. Though virtual calibration may be used, its simulation accuracy is still decided by measurement in model updating.

As far as the former is concerned, 4101 points are selected and distributed around the trajectory sphere so that they partition the domain into 2004 spherical triangles with each edge near equal to 11 m. Then an arbitrary triangle is selected with three apexes and three midpoints, as shown in Figure 7(a). For any point within the triangle, strokes based on FE simulation can be obtained as real values. At the same time interpolation strokes can be calculated as well. The difference between them is regarded as the interpolation error. The error is calculated based on an RMS statistics of 2225 stroke differences. Several paraboloid apexes (red star) are tried (in spherical coordinates), and their corresponding interpolation errors are shown in the figure. The figure shows the results of spatial interpolation when

the temperature is 10°C. Similar interpolation results can be obtained in temperature domain.

The errors seem slightly bigger than anticipated compared with the calibration error of the latter. A method for improvement may come out. As an actuator drives its down-tied cable and therefore a paraboloid deformation off the base sphere. Its absolute stroke consists of three parts. One is the stroke when it stands on the base sphere. The second is a distance as it leaves for the object paraboloid shape along its tension direction, usually radial. This part can be calculated geometrically once the paraboloid is determined. According to Jiang et al. (2017), it can be written as

$$d(\theta) = \rho(\theta) - 300. \quad (12)$$

Here  $\rho(\theta)$  is the polar equation of paraboloid. The origin of polar coordinate frame is the spherical center and the symmetric axis of paraboloid is set as the polar axis. The third part is a few influences such as elasticity of cable, temperature, gaps and so on. It is small compared with the former two parts and hard to determine completely by computation. This part represents a compensation of the geometric calculation. Let us rewrite the absolute actuator stroke corresponding to a given paraboloid deformation as follows

$$S_C(P, T) = S(P, T) - S_0 - S_G(P). \quad (13)$$

Here  $S(P, T)$  is the absolute stroke vector;  $S_G(P)$  represents the second part given in Equation (12) and  $S_C(P, T)$  is the third part. The improved method will remove all the known factors and leave only the third part  $S_C(P, T)$  for interpolation. Based on the improved method, the interpolation error is again tried on the same triangle and interpolation points, as shown in Figure 7(b). This shows that the errors reduce greatly as much as only 10%~15% of the initial values. So Equation (13) is finally used to form a calibration table of standard paraboloids.

As far as the latter is concerned, the real shape accuracy of the base sphere and standard paraboloids are the main focus. Basically that of the base sphere is more important in that it is the baseline, so higher accuracy is demanded. There are a few conditions on the calibration of base sphere. It is usually during a cloudy morning of summer with air temperature nearly to 20°C and before sunrise to avoid an uneven distribution. It should be an average value of several times to reduce the measurement error as much as possible. The final shape error should not be larger than 2.0 mm RMS, compared with about 1.5 mm RMS of the measurement error. In the case of the calibration of standard paraboloids, though the condition is not so strict, its final shape error should be confined within 3 mm RMS. In the case of virtual calibration, the value should be further constrained, leaving error space for model updating. With

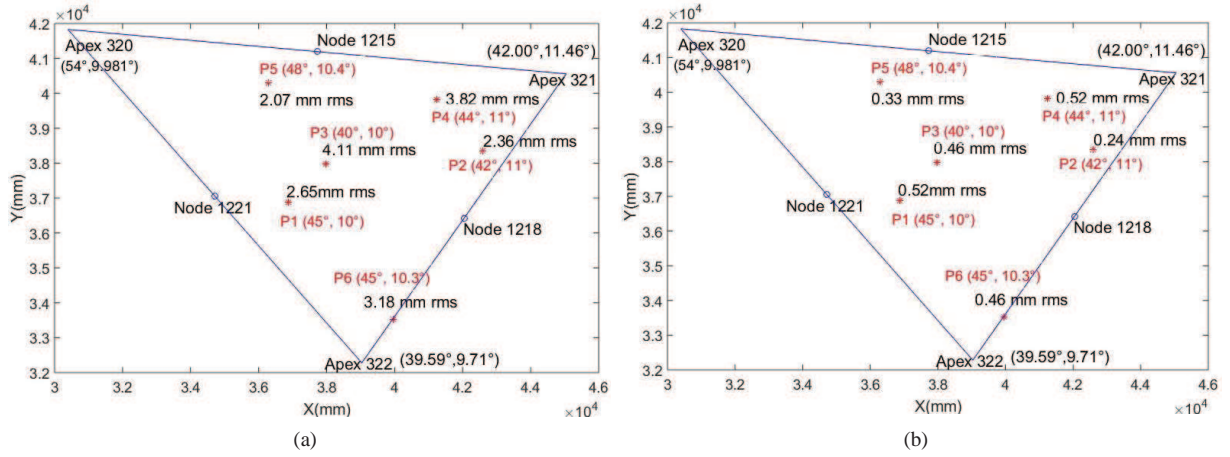


Fig. 7 Comparison of interpolation error between two methods. (a) Initial method; (b) Improved method.

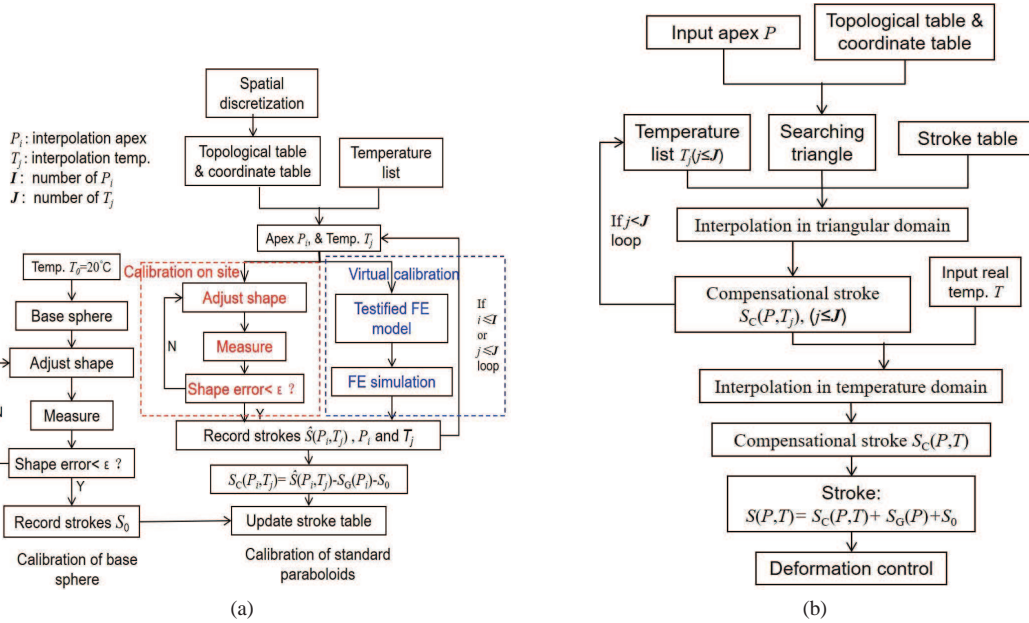


Fig. 8 Flow chart of open-loop control. (a) Build database; (b) Interpolation.

regarding to the limit of above errors and other possible errors, the final control error is estimated less than 5 mm RMS for any paraboloid shape deformed by the cable-net.

### 3.7 Considerations on Deformation Safety

Generally, the paraboloid deformation happens within the 500 m aperture if its zenith angle is less than  $26.4^\circ$ . As its zenith angle further increases, some parts of the 300 m illumination area begin to spill from the 500 m aperture. As a result, the cable nodes at the outermost margin cannot move to the paraboloid shape as expected due to the limit of the ring girder. At last the corresponding down-tied cables usually have zero tensions. So, large-zenith paraboloid deformation is different. The cable nodes at the outermost

margin are not required to track the paraboloid shape any more. The corresponding down-tied cables are required to keep at least a threshold value of prestress. Otherwise some dangers like fatigue of cables and collision of reflector elements may exist. Another case is extremely low temperature which may cause abnormally high stresses of some cables. On such occasions, the corresponding cable nodes are also not required to track the paraboloid shape exactly any more. Therefore the cable stresses are expected to decrease within the safety range.

It is clear that close-loop control or a simple geometric calculation is very hard to take the above two cases into consideration. It is lucky that calibration of standard paraboloids provides the solution. Before calibration on site, mechanical simulation is done to obtain an initial s-

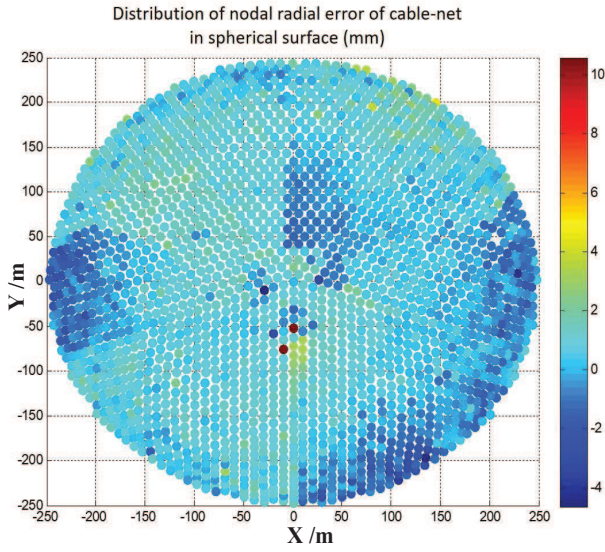


Fig. 9 Calibrated shape error of the base sphere (1.7 mm RMS).

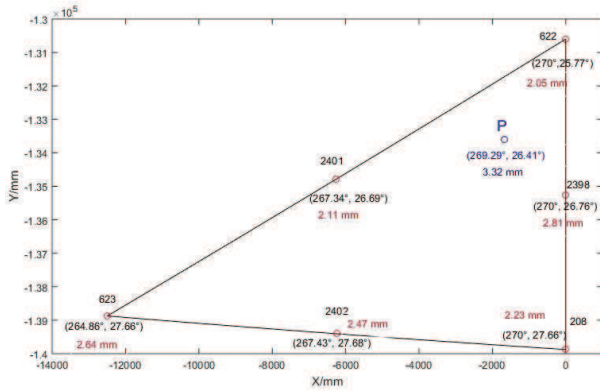


Fig. 10 Triangular domain for the interpolation of paraboloid (269.29°, 26.41°) and the measured shape errors (RMS) of six standard paraboloids.

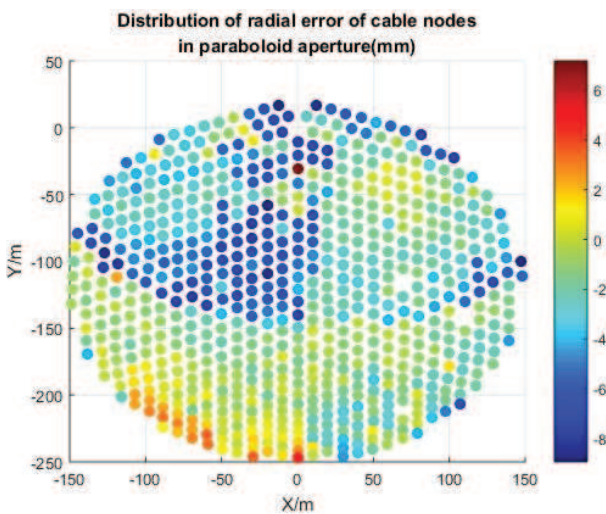


Fig. 11 Measured shape error of the paraboloid (269.29°, 26.41°).

tatus regarding the deformation safety. Simulation can be continued after the calibration to assess deformation safety. For virtual calibration, the simulation result itself has already considered deformation safety.

### 3.8 Overview of Open-loop Control

The whole work is made of two phases. The first is to build the database for interpolation following this method. It devotes to a lot of important hard work and may take a long time. The second is involved in programming of the above control algorithm, including searching the spherical triangle which the interpolation point belongs to. Figure 8 shows the total flow chart. It is worth noting that a very important step is the calibration of the base sphere on site. As the baseline of absolute actuator stroke, it is only available via measurement on site. Furthermore, the calibration temperature  $T_0$  is fixed on 20°C, a value that happens frequently in local weather and under which the cables are manufactured as well. During the calibration of standard paraboloids, either method may be available. At the beginning, more focus may be put on the calibration on site in that it can provide measurement data for updating the finite element model as well. Then virtual calibration are applied for much more other standard paraboloids and other discrete temperatures that are not easy to catch during the calibration.

### 4 VERIFICATION OF CONTROL ACCURACY

Our algorithm was tested on site. Here only calibration on site was available. The laser measurement was used for calibrations and the next verification. First, the shape accuracy of the base sphere was calibrated. Since it is the baseline of all calculations in the open-loop algorithm, the calibration is strictly done at dawn of summer just before the sunrise when the temperature is close to 20°C and smoothly distributed. Furthermore the calibration was repeated at least three times to get arithmetic average to reduce the measurement error as possible. Though in the calibration there might be some abnormal actuators that could not fulfill the stroke adjustments, the number was small and it did not affect the calibration greatly. They could be left for the next calibration. Figure 9 shows the final shape error, about 1.7 mm RMS as a statistic result of 2225 positions of cable nodes, less than the required 2 mm RMS. Second, six standard paraboloids building a spherical triangular domain were calibrated for the next interpolation. It took 3 days in January to finish the calibrations so that the ambient temperature was about 6°C for each calibration. The required error for paraboloid calibration is less than 3 mm RMS. Figure 10 shows No. of the six standard paraboloids, their

positions and their measured actual shape error (RMS). Finally an arbitrary paraboloid with the spherical coordinate  $(269.29^\circ, 26.41^\circ)$  was selected in the triangular domain for the interpolation and the next structural deformation on 2019 Jan. 27. The local temperature was the same  $6^\circ\text{C}$ . The total time needed for calculation was also tested on the platform of MATLAB software, about 100 ms, less than the required 500 ms. The time is not only obviously shorter than the measurement time, but also obviously less than the fastest simulation time by finite element analysis, about 40 – 50 s. The 2225 calculated strokes were then sent to PLC for the structural deformation. Its actual shape error is shown in Figure 10 and the error distribution is shown in Figure 11,  $\sim 3.32$  mm RMS, less than the requirement of 5 mm RMS. It proves that the algorithm works.

## 5 CONCLUSIONS

An open-loop control algorithm is put forward for the deformation control of the active reflector system of FAST. The method is based on a calibration database and interpolation in 2D spatial domain and temperature domain respectively.

The algorithm has three main steps. First, discretization is done to get the spherical triangles and the standard paraboloids on the trajectory sphere. Similarly the discrete temperatures are selected in temperature domain. Second, calibration is done for the base sphere and standard paraboloids to build database for interpolation. Finally, interpolation is done first in the spatial domain and then in the temperature domain to get the 2225 actuator strokes mapping to a given paraboloid deformation.

The algorithm is completely independent of real-time measurement of cable nodes so that it has advantage of working all-weather and no additional EMI. Furthermore, its control accuracy can be effectively improved via reasonable layout of standard paraboloids and increasing calibration accuracy. Meanwhile, deformation safety is effectively considered via calibration.

**Acknowledgements** This research is supported by the National Natural Science Foundation of China (No. 11573044), the West Light Foundation of Chinese Academy of Sciences, and the Open Project Program of the Key Laboratory of FAST, NAOC, Chinese Academy of Sciences. We thank Bo Zhang and Fei Zhao for their help in typesetting works.

## References

- Ahlberg, J. H., Nilson, E. N., & Walsh, J. L. 1967, *Mathematics in Science and Engineering*, 38 (New York and London: Academic Press Inc.)
- Gan, H. Q. 2010, *Reflector Tolerance Calculation of FAST and Front End of Radio Telescope*, PhD Thesis (Beijing: Graduate University of Chinese Academy of Sciences)
- Jiang, P., Wang, Q., & Zhao, Q. 2013, *Engineering Mechanics*, 30, 400 (in Chinese)
- Jiang, P., Li, Q. W., & Nan, R. D. 2017, *RAA (Research in Astronomy and Astrophysics)*, 17, 99
- Jiang, P., Yue, Y., Gan, H., et al. 2019, *Science China Physics, Mechanics & Astronomy*, 62, 959502
- Nan, R. D. 2006, *Science in China: Series G Physics, Mechanics and Astronomy*, 49, 129
- Qian, H. L. 2007, *Theoretical and Experimental Research on Supporting Structure of FAST Reflector*, PhD Thesis (Harbin: Harbin Institute of Technology)
- Qiu, Y. H. 1998, *Chinese Astronomy and Astrophysics*, 22, 361
- Shen, S. Z., Fan, F., & Qian, H. L. 2010, *Journal of Building Structures*, 31, 1 (in Chinese)
- Wang, X.-C. 2003, *Finite Element Method* (Tsinghua University Press) (in Chinese)
- Xue, J.-X., Wang, Q.-M., Gu, X. D., et al. 2015, *Optics and Precision Engineering*, 23, 2051 (in Chinese)
- Zhu, L., & Zhang, Z. 2010, *Metrology Test Technology and Verification*, 20, 7 (in Chinese)
- Zhu, L. 2012, *E-science Technology and Application*, 3, 67
- Zhu, Z., Liu, F., Zhang, L., et al. 2017, *Spatial Structures*, 23, 3 (in Chinese)